CFD-BASED HYDRODYNAMIC ANALYSIS FOR A SHIP SAILING ALONG A BANK IN RESTRICTED WATERS

M G Zhou, **S J Ma** and **Z J Zou**, Shanghai Jiao Tong University, China.

SUMMARY

For a ship navigating along a bank in restricted waters, it is usually accompanied by obvious bank effect which may cause ship-bank collision. In order to avoid collision, it is necessary to provide control force and moment by using control devices such as a rudder. In this paper, CFD method is applied to numerically simulate the viscous flow around a ship appended with a rudder sailing along a bank. Systematical simulations are carried out for the hull-rudder system with different rudder angles at different ship-bank distances and water depths. The flow field features and the hydrodynamic forces of the hull-rudder system are obtained and analysed. This study is of significance for revealing the physical mechanism behind the bank effect and providing guidance for ship steering and control in restricted waters.

1. INTRODUCTION

During the last decades, the main dimensions of ships have been increasing constantly, but the waterways in which the ships sail are seldom expanded at the same rate. As a result, the waterways become restricted and the ship behaviour will be more influenced by the bank effect and/or shallow water effect. For a ship sailing along a bank, the bank effect is caused by the pressure difference between the port side and starboard side due to the asymmetrical flow around the ship. Usually, a lateral force directing to the bank and a yaw moment pushing the stern towards the bank will be induced on the ship. This bank effect has a harmful impact on ship manoeuvring properties and, in the worst cases, may lead to ship-bank collision.

In order to keep the ship sailing along the required course and to avoid ship-bank collision, control forces have to be provided. One of the most commonly used devices to provide such control forces is rudder. However, these control forces are limited. When the forces supplied by the rudder fail to control the ship under the influence of bank effect, the ship may come into an uncontrollable state and a collision accident may happen. Therefore, to ensure the safe navigation of ships in the restricted waters, the flow field and hydrodynamic characteristics of the hull-rudder system must be properly understood.

In the past decades, many investigations on bank effect have been carried out, both experimentally and numerically. Norrbin (1974, 1985)[1,2] carried out a series of experiments for a tanker model moving along three different banks and proposed empirical formulas to estimate the hydrodynamic forces for flooded, vertical and sloping banks. Renilson and Munro (1989)[3] performed the model test for a ship with a vertical bank and a bank sloping at 45° with the ratio of water depth to ship draft being 1.5. Ch'ng et al. (1993)[4] conducted a series of model tests and developed an empirical formula to estimate the bank-induced sway force and yaw moment for a ship handling simulator. Li et al. (2001)[5] continued Norrbin's investigations and tested the bank effect in extreme conditions for three different hull forms (tanker, ferry and catamaran). The influence of ship speed, propeller loading and bank inclination was evaluated. Duffy (2002)[6] dealt with the effect of lateral banks for ships operating in a port environment through a series of model tests and derived regression formulas of resultant sway force and yaw moment acting on the ship. Vantorre et al. (2003)[7] carried out systematic captive model tests to investigate the influence of the main parameters on the ship-bank interaction and proposed new empirical formulas. Lataire and Vantorre (2008)[8] conducted model tests to study bank effects induced by irregular bank geometries. A mathematical model for the longitudinal force, sway force, yaw moment and sinkage was formulated based on these tests.

Although experimental methods and empirical formulas are widely used for the bank effect prediction, they usually fail to provide detailed information of the flow field, and hence are unable to explain the flow-related physical mechanism behind the bank effect. In view of this, people turn to numerical methods, especially in the last decade, as CFD-based method has become a powerful tool for numerical study on the hydrodynamic problems related to ship manoeuvrability. Miao et al. (2008)[9] studied the case of a ship traveling in a rectangular channel. The sway force, yaw moment and wave pattern were numerically predicted based on Dawson's method. Yao and Zou (2010)[10] applied a 3-D panel method to investigate the bank effect for a ship travelling along a bank. With respect to the application of CFD method for viscous flow, Lo et al. (2009)[11] performed a series of numerical simulations of the KRISO 3600 TEU container ship model navigating in close proximity to a lateral bank by using commercial FLOW-3D software. The influences of ship speed and ship-bank distance on the magnitude and temporal variation of the yaw angle and sway force were reported. Wang et al. (2010)[12] studied the viscous flow and predicted the hydrodynamic forces on a ship sailing along a bank by using the FLUENT software. The numerical study was carried out for a Series 60 ship with C_B=0.6. Zou et al. (2011)[13] applied the SHIPFLOW software to investigate the bank effect on a tanker moving straight ahead at low speed in a canal. V&V (Verification and Validation) studies were also carried out.

Most of the previous studies mainly focused on the influence of the bank effect without taking the influence of rudder effect into consideration. Eloot et al. (2007)[14] considered a ship appended with propeller and rudder, and presented a methodology to evaluate the controllability of the ship navigating in a restricted channel by comparing the available control forces from rudder with the forces induced by environmental disturbances such as bank effect. In the present paper, the viscous flow around a ship appended with a rudder and moving along a bank in shallow water is numerically simulated by using the CFD software FLUENT to solve the Reynolds-Averaged Navier-Stokes (RANS) equations. A series of calculations are carried out for the hull-rudder system at different ship-bank distances, rudder angles and water depths. The sway force and yaw moment acting on the hull-rudder system are calculated. Based on the numerical results, systematical analysis on the flow field and hydrodynamics is conducted and the ship behaviours in restricted waters are evaluated.

2. MATHEMATICAL FORMULATIONS AND NUMERICAL SOLUTION

As shown in Figure 1, a ship appended with a rudder sailing ahead with a constant speed along a vertical bank is considered. A right-handed Cartesian coordinate system is adopted. The origin O is located at the intersection of the mid-ship section, the ship's longitudinal centre plane and the undisturbed free surface; x-axis is pointing forward and y-axis is pointing to the starboard. δ is the rudder angle which is positive when turning to the starboard side; X, Y and N are the components of hydrodynamic force and moment acting on the hull-rudder system, respectively.

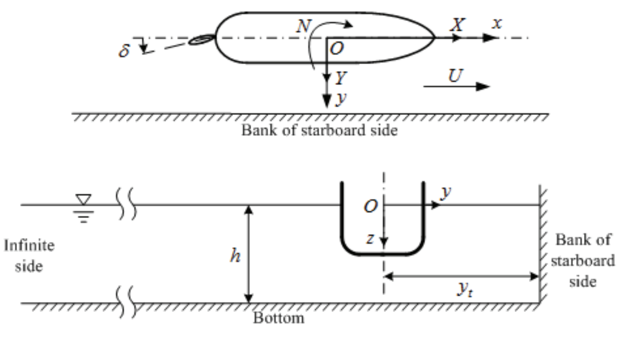

Figure 1 Sketch map for a ship sailing along a vertical bank in shallow water

2.1 GOVERNING EQUATIONS

The governing equations of the viscous flow around the hull-rudder system are the Reynolds-averaged continuity equation and momentum equations which are given as follows[15][16]:

$$\begin{cases} \dfrac{\partial u_i}{\partial x_i} = 0 \\ \rho \dfrac{\partial u_i}{\partial t} + \rho u_j \dfrac{\partial u_i}{\partial x_j} = -\dfrac{\partial p}{\partial x_i} + \dfrac{\partial}{\partial x_j}\left(\mu \dfrac{\partial u_i}{\partial x_j} - \rho \overline{u_i' u_j'} \right) \end{cases} \tag{1}$$

where x_i is the ith component of coordinate system, u_i and u_j are the mean velocity components, p is the mean pressure, μ is the viscosity coefficient, $-\rho\overline{u_i' u_j'}$ is the Reynolds stress.

Standard k-ε turbulence model is adopted to close the governing equations:

$$\begin{cases} \dfrac{\partial(\rho k)}{\partial t} + \dfrac{\partial(\rho k u_i)}{\partial x_i} = \dfrac{\partial}{\partial x_j}\left[\left(\mu + \dfrac{\mu_t}{\sigma_k}\right)\dfrac{\partial k}{\partial x_j}\right] + G_k - \rho\varepsilon \\ \dfrac{\partial(\rho\varepsilon)}{\partial t} + \dfrac{\partial(\rho\varepsilon u_i)}{\partial x_i} = \\ \qquad \dfrac{\partial}{\partial x_j}\left[\left(\mu + \dfrac{\mu_t}{\sigma_\varepsilon}\right)\dfrac{\partial \varepsilon}{\partial x_j}\right] + C_{1\varepsilon}\dfrac{\varepsilon}{k}G_k - C_{2\varepsilon}\rho\dfrac{\varepsilon^2}{k} \end{cases} \tag{2}$$

where the expressions of the terms and the values of the constants are as follows[16]:

$$k = \frac{\overline{u_i' u_i'}}{2}, \quad \varepsilon = \frac{\mu}{\rho}\overline{\left(\frac{\partial u_i'}{\partial x_k}\right)\left(\frac{\partial u_i'}{\partial x_k}\right)}, \quad \mu_t = \rho C_\mu \frac{k^2}{\varepsilon}$$

$$G_k = \mu_t\left(\frac{\partial u_i}{\partial x_j} + \frac{\partial u_j}{\partial x_i}\right)\frac{\partial u_i}{\partial x_j}, \quad C_{1\varepsilon} = 1.44, \quad C_{2\varepsilon} = 1.92$$

$$C_\mu = 0.09, \quad \sigma_k = 1.0, \quad \sigma_k = 1.3$$

2.2 BOUNDARY CONDITIONS

The computational domain and its boundaries are shown in Figure 2. The computational domain is bounded by the hull and rudder surfaces, the water bottom, the free surface, the bank on the starboard side, the far field boundary on the port side, as well as the fictitious boundaries upstream and downstream (inlet and outlet boundaries). The computational domain and the hull-rudder system are regarded as stationary, while an inflow of velocity $-U$ is imposed, where U is the ship speed.

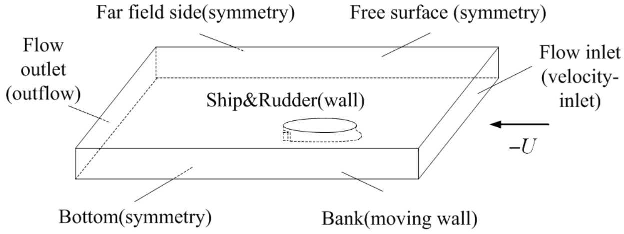

Figure 2 Computation domain and boundary conditions

In the numerical study, the inlet boundary is 1.0L ahead of the bow, where L is the ship length. The outlet boundary is 3.0L downstream of the stern. The far field boundary is

1.5L away from the port side of the hull. In the present study, the ship speed is assumed to be low, so that the influence of free surface elevation on the hydrodynamic forces is negligible, and the upper boundary can be replaced by the undisturbed free surface.

The boundary conditions are set as follows[17]: A velocity-inlet condition is imposed on the inlet and an outflow condition is imposed on the outlet; On the far field boundary, a symmetry condition is imposed; On the undisturbed free surface, a symmetry condition is imposed; On the hull and rudder surfaces, no-slip wall condition is imposed; According to the principle of relative motion, the bank and bottom are moving along with the fluid with velocity $-U$, and no-slip moving wall condition is imposed on them.

2.3 NUMERICAL SOLUTION

The CFD software FLUENT is used in this paper with FVM (Finite Volume Method) to discretize the governing equations[18]. The pressure equation is discretized by second order scheme, while the momentum equations and turbulence equations are discretized by second order upstream scheme to guarantee the calculation accuracy. The SIMPLEC algorithm is applied to solve the velocity-pressure coupling problem. Hybrid unstructured mesh with multi-blocks is utilized: the blocks containing the bow, stern and rudder are mainly meshed with tetra element, and the other blocks are meshed with hex element. Meanwhile, finer mesh is used near the bow and stern. Standard Wall Function treatment is adopted to simulate the flow near the wall-condition boundaries, and the y+ value there is limited in a range of 30 to 300.

3. CASE FOR STUDY

Numerical calculations are conducted for a KCS model appended with a semi-balanced horn rudder[19]. The principal particulars of the hull and rudder are listed in Table 1.

Table 1 Principal particulars of the hull and rudder

Particulars	Full-scale	Model
Hull		
Length L_{pp} (m)	230	5.1111
Width B (m)	32.2	0.7156
Draft T (m)	10.8	0.2400
Displacement ∇(m^3)	52030	0.8777
Block coefficient C_B	0.65	0.65
LCB (%), fwd+	−1.48	−1.48
Rudder		
Rudder area A_R(m^2)	54.45	0.0269

In order to get deeper insight into the bank effect and rudder effect, different h/T, δ and y_t/B are chosen to investigate their influences on hydrodynamic forces of the hull-rudder system. The detailed calculation conditions are given in Table 2, where *inf* stands for the case without bank. For each h/T, the rudder angle varies from −35° to +35°, and y_t/B varies from 1.00 to 5.00 and *inf*.

Figure 3 shows the mesh generated in the bow and stern regions with both hex elements and tetra elements.

4. NUMERICAL RESULTS AND ANALYSIS

4.1 ANALYSIS OF HYDRODYNAMICS UNDER BANK EFFECT AND RUDDER EFFECT

In this subsection, analysis of the hydrodynamics under bank effect and rudder effect is carried out based on the calculation results of Group 1 in Table 2.

Table 2 Calculation conditions for the numerical study

Items	h/T	U (m/s)	Fr	Frh	Rn	δ (°)	y_t/B
Group 1	1.5	0.6135	0.0866	0.3265	3.12×10^6	0, ± 5, ± 10, ± 15, ± 20, ± 25, ± 30, ± 35	1.00, 1.50, 2.00, 2.25, 2.50, 3.00, 4.00, 5.00, *inf*
Group 2	2.0			0.2827			

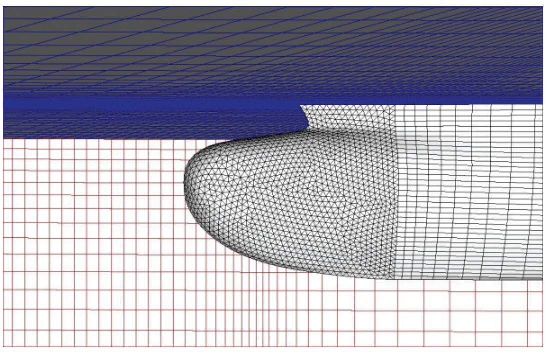

(a) grid in the bow region

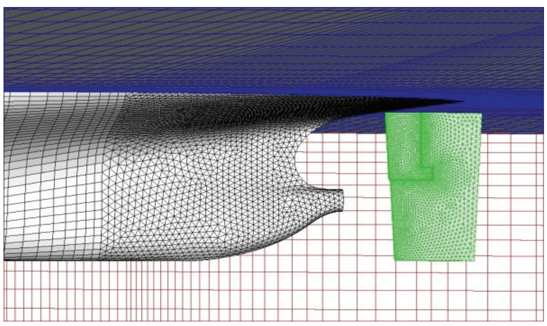

(b) grid in the stern region

Figure 3 Mesh generated for calculation

4.1(a) Analysis of Flow Field

For the ship navigating along the bank with and without a rudder angle, the flow fields are quite different. As a result, the hydrodynamic features of the hull-rudder system also differ a lot. Here the flow field features are studied under the following three conditions.

Without rudder angle

As an example, Figure 4 and Figure 5 show respectively the velocity distribution on the undisturbed free surface and the pressure distribution on the ship and rudder for y_t/B=2.5 and δ =0°, where 'P' denotes the port side and 'S' denotes the starboard side. As shown in Figure 4, the flow velocity near the starboard side of the hull is larger than that near the port side. In Figure 5(a), the pressure on the starboard side of the hull is smaller than that on the port side throughout the ship length except near the bow region; In Figure 5(b) the pressure on the port side and starboard side of the rudder is nearly the same. The asymmetrical pressure distribution on the ship results in a force pointing to the bank and a moment pushing the stern to the bank, which accounts for the bank effect.

As an example, the pressure distributions on the ship and rudder for y_t/B=2.5 and δ =15° are depicted in Figure 6. It can be seen that with the positive rudder angle, the flow field is influenced in two aspects: the pressure distribution on the starboard side of the hull is still smaller than that on the port side, but this asymmetrical phenomenon is less severe than that without rudder angle; On the other hand, the pressure on the starboard side of the rudder is larger than that on the port side. Both of these two phenomena indicate that the rudder effect counteracts the bank effect to some extent, which may result in a smaller sway force pointing to the bank and a smaller moment pushing the stern to the bank. If the rudder angle is large enough, the sway force may point away from the bank and the yaw moment may push the stern off the bank.

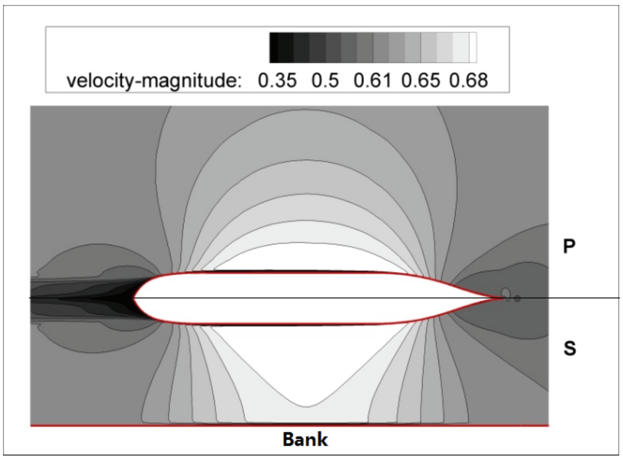

Figure 4 Velocity distribution on the undisturbed free surface (y_t/B=2.5, δ =0°; h/T=1.5)

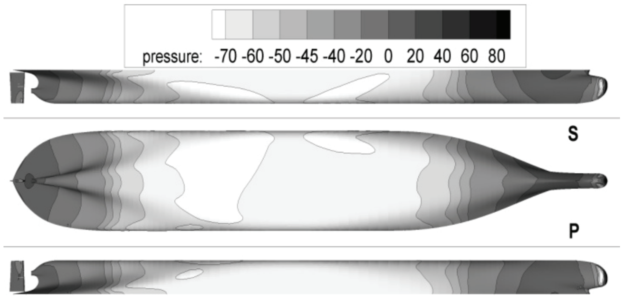

(a) on the ship

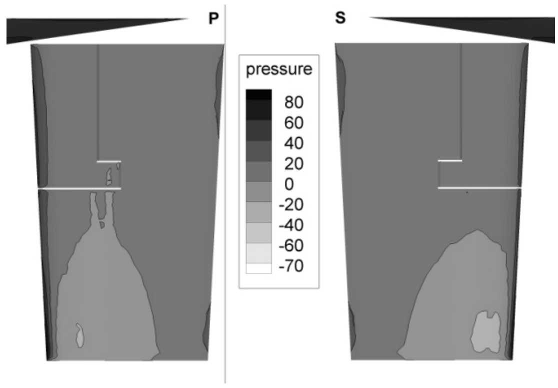

(b) on the rudder

Figure 5 Pressure distributions on the ship and rudder (y_t/B=2.5, δ =0°; h/T=1.5)

With positive rudder angle (to starboard side)

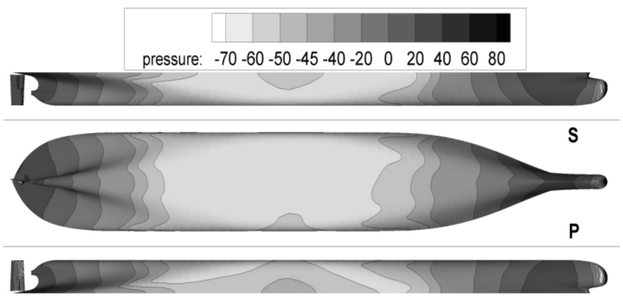

(a) on the ship

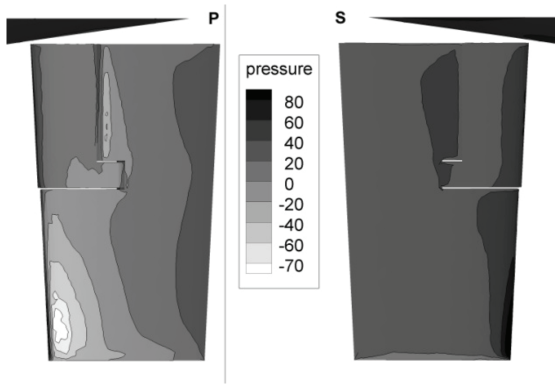

(b) on the rudder

Figure 6 Pressure distributions on the ship and rudder (y_t/B=2.5, δ =15°; h/T=1.5)

With negative rudder angle (to port side)

Take the case of y_t/B=2.5 and δ =−15° as example, the pressure distributions on the ship and rudder are shown in Figure 7. It can be seen from Figure 7 that the pressure distribution on the ship is similar to that in Figure 5, but with more significant asymmetrical phenomenon; meanwhile, the pressure on the starboard side of the rudder is smaller than that on the port side. Both of these two phenomena indicate that the rudder effect aggravates the bank effect, which may result in a larger sway force pointing to the bank and a larger moment pushing the stern to the bank in comparison with the case without rudder angle.

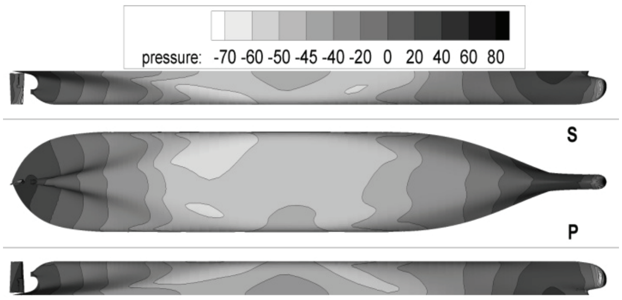

(a) on the ship

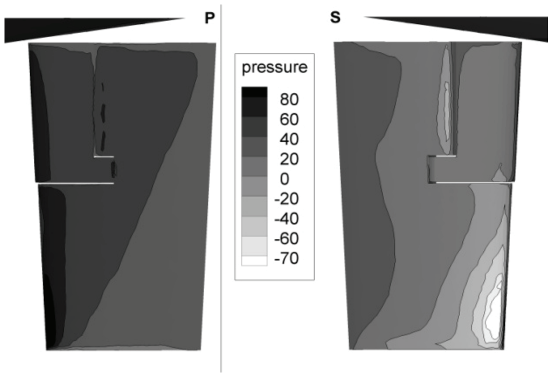

(b) on the rudder

Figure 7 Pressure distributions on the ship and rudder (y_t/B=2.5, δ =−15°; h/T=1.5)

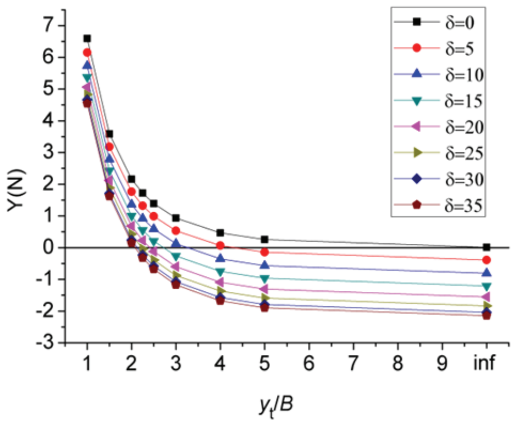

(a) with rudder to starboard side

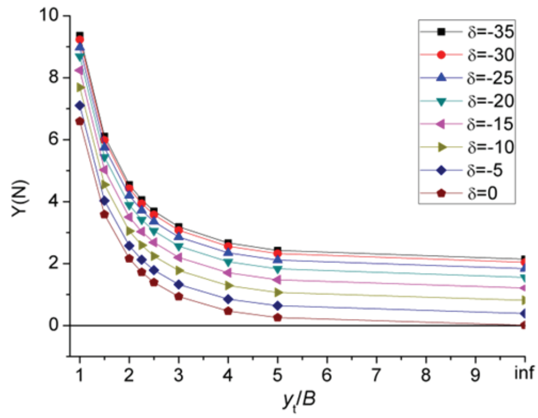

(b) with rudder to port side

Figure 8 Sway force versus ship-bank distance at different rudder angles

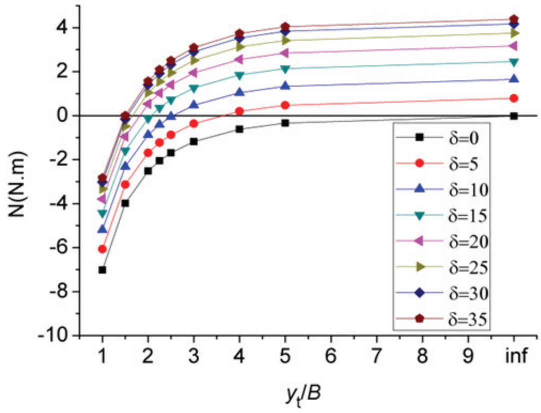

(a) with rudder to starboard side

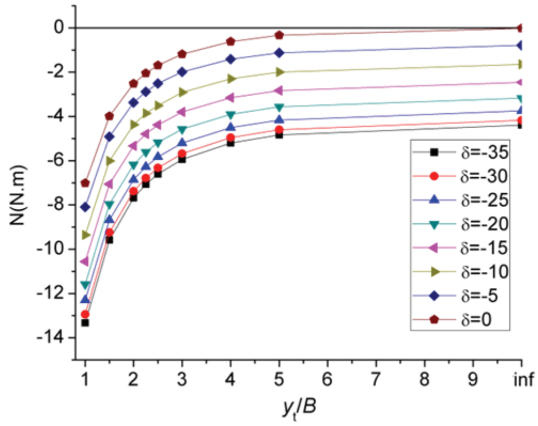

(b) with rudder to port side

Figure 9 Yaw moment versus ship-bank distance at different rudder angles

4.1(b) Analysis of Hydrodynamic Forces

Figure 8 and Figure 9 show the sway force and yaw moment acting on the hull-rudder system changing with ship-bank distance at different rudder angles. Obvious bank effect can be observed: the sway force becomes larger when the ship gets closer to the bank, and will increase sharply when the ship-bank distance is very small; the yaw moment changes in a similar way.

Figure 10 and Figure 11 depict the sway force and yaw moment acting on the hull-rudder system changing with rudder angles at different ship-bank distances. It can be seen that when the ship is not too close to the bank, with the rudder angle changing from negative to positive, the sway force changes from positive (suction force) to negative (repulsive force), and the yaw moment changes from negative (stern suction) to positive (bow suction). This indicates that with the rudder angle changing from negative to positive, the force and moment generated by the rudder can counteract the bank effect. However, when ship is very close to the bank, the resultant sway force remains positive (suction force) and yaw moment remains negative (stern suction) regardless of the rudder angles. In this situation, the control effect of the rudder is not large enough to offset the bank effect.

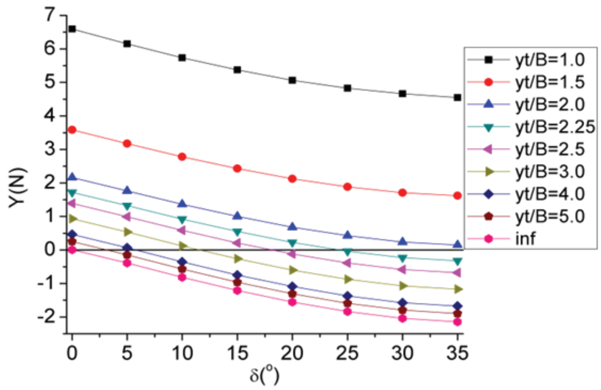

(a) with rudder to starboard side

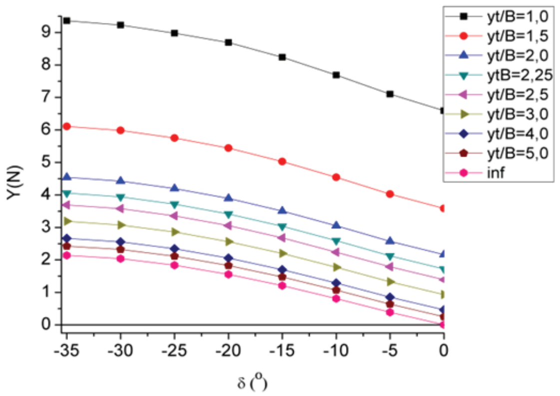

(b) with rudder to port side

Figure 10 Sway force versus rudder angle at different ship-bank distances

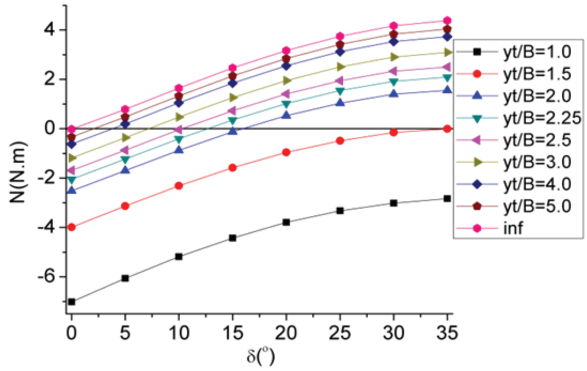

(a) with rudder to starboard side

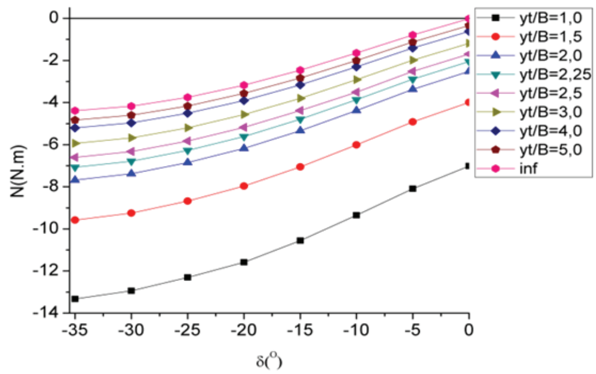

(b) with rudder to port side

Figure 11 Yaw moment versus rudder angle at different ship-bank distances

In order to predict the navigation safety under certain condition more conveniently, curves of $Y(y_t,\delta)=0$ and $N(y_t,\delta)=0$ are obtained by interpolation, as shown in Figure 12. These curves indicate the critical state that the bank effect is balanced by rudder effect. They reflect important hydrodynamic features of the hull-rudder system sailing along the bank. It can be seen that the whole rectangular area in Figure 12 is divided by the curves $Y(y_t,\delta)=0$ and $N(y_t,\delta)=0$ into three zones representing three typical situations:

(1) **Zone A** for *Y*<0 and *N*>0, where the ship has a tendency to move away from the bank and the yaw motion tends to push the bow to bank;

(2) **Zone B** for *Y*>0 and *N*>0, where the ship has a tendency to move towards the bank and the yaw moment tends to push the bow to the bank;

(3) **Zone C** for *Y*>0 and *N*<0, where the ship has a tendency to move toward to the bank and the yaw moment tends to push the stern to the bank.

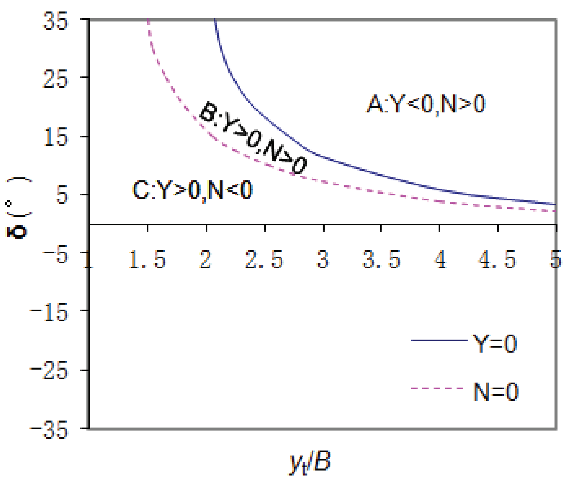

Figure 12 Curves indicating the critical state

4.2 HYDRODYNAMIC ANALYSIS UNDER DIFFERENT WATER DEPTHS

In order to investigate the influence of water depth on the hydrodynamic characteristics of the hull-rudder system, analysis is carried out by comparing the results of Group 2 with Group 1 in Table 2.

4.2(a) Analysis of Flow Field When h/T=2.0

Here the calculation results in Group 2 are presented diagrammatically. Similar as in Section 4.1(a), three different cases are considered and the same rudder angle is selected in each case for comparison purpose.

Without rudder angle

Figure 13 and Figure 14 show the velocity distribution on the undisturbed free surface and the pressure distributions on the ship and rudder for y_t/B=2.5, δ =0° and h/T=2.0. It can be seen from these figures that the bank effect can also be observed when h/T=2.0, and the main flow features are similar with those shown in Figure 4 and Figure 5 when h/T=1.5. However, compared with Figure 4 and Figure 5, the velocity distribution and pressure distribution are more symmetrical than those when h/T=1.5. This will result in a smaller sway force pointing to the bank and a smaller yaw moment pushing the stern to the bank. One conclusion that can be drawn for the current case is that the deeper the water depth, the weaker the bank effect.

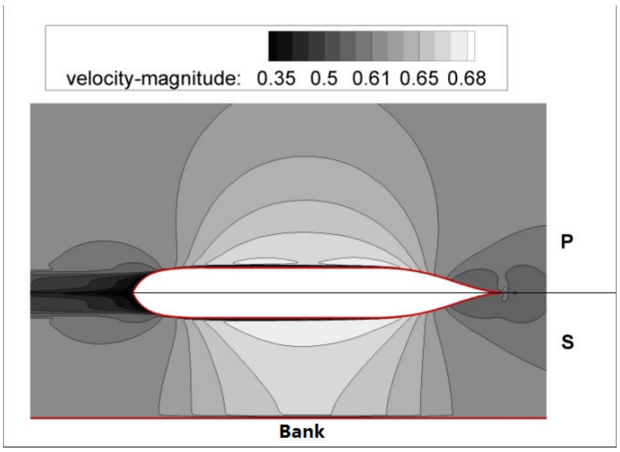

Figure 13 Velocity distribution on the undisturbed free surface (y_t/B=2.5, δ =0°; h/T=2.0)

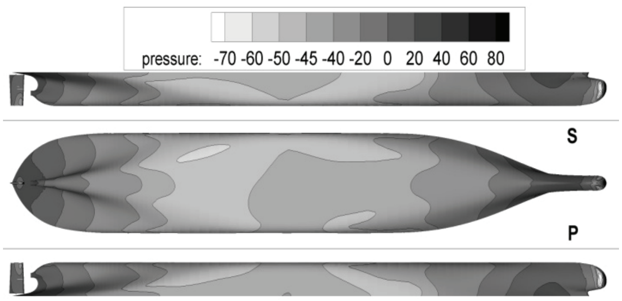

(a) on the ship

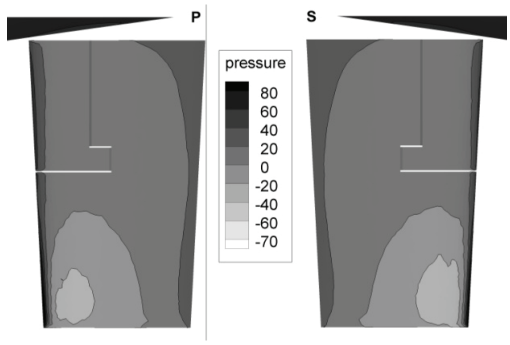

(b) on the rudder

Figure 14 Pressure distributions on the ship and rudder (y_t/B=2.5, δ =0°; h/T=2.0)

With positive rudder angle (to starboard side)

As an example, Figure 15 shows the pressure distributions on the ship and rudder for y_t/B=2.5, δ =15° and h/T=2.0. Comparing Figure 15(a) with Figure 6(a), it can be seen that the pressure distribution on the hull is more symmetrical than that when h/T=1.5; Moreover, the asymmetrical pressure distribution on the rudder surface is more severe in Figure 15(b) than that in Figure 6(b). These indicate that the bank effect becomes weaker while the rudder effect becomes stronger in deeper water, thus the rudder effect can counteract the bank effect to a larger extent. One possible explanation for the strengthening of the asymmetrical pressure distribution on the rudder surface is that the velocity in the hull's wake around the rudder increases when the water becomes deeper.

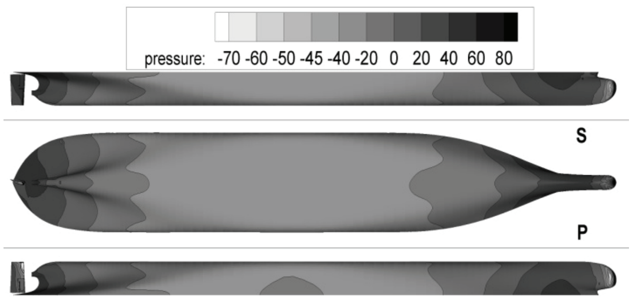

(a) on the ship

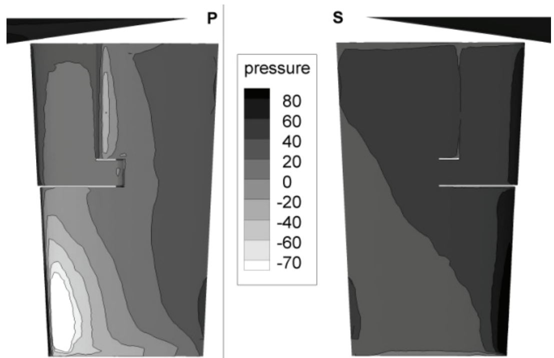

(b) on the rudder

Figure 15 Pressure distributions on the ship and rudder (y_t/B=2.5, δ =15°; h/T=2.0)

With negative rudder angle (to port side)

Figure 16 shows the pressure distributions on the ship and rudder for y_t/B=2.5, δ =−15° and h/T=2.0. It can be seen that a more symmetrical pressure distribution on the hull is revealed in Figure 16(a) compared with Figure 7(a); while the asymmetrical pressure distribution on the rudder surface is more significant in Figure 16(b) than that in Figure 7(b). The explanation for these phenomena is similar to that when the rudder angle is positive. Since the rudder effect becomes stronger while the bank effect becomes weaker in this case, as a synthetical result of these effects, the total hydrodynamic force and moment can be either larger or smaller than those when h/T=1.5.

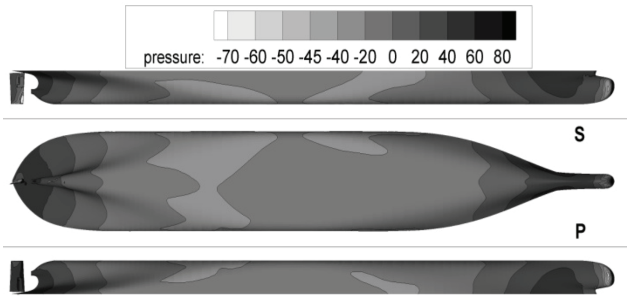

(a) on the ship
(b)

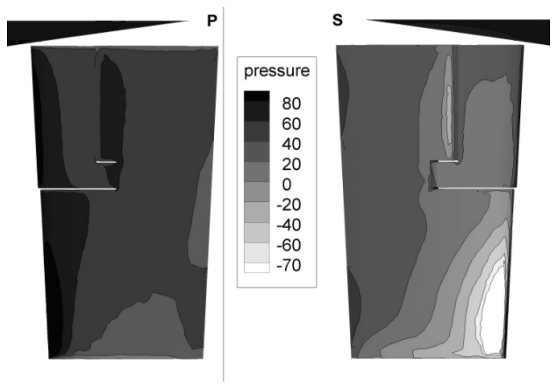

(b) on the rudder

Figure 16 Pressure distributions on the ship and rudder (y_t/B=2.5, δ =−15°; h/T=2.0)

4.2(b) Analysis of Hydrodynamic Forces When h/T=2.0

As examples, the force and moment on the hull-rudder system versus the ship-bank distance under different water depths with rudder angle δ=0°, 15° and −15° are shown in Figure 17, Figure 18 and Figure 19, respectively.

When δ=0°, it can be seen from Figure 17 that the sway force and yaw moment at deeper water are smaller than those at shallower water except the case without the bank. This indicates that the bank effect becomes weaker with the increase of water depth. It can be confirmed by the flow field comparisons (Figure 4 and Figure 5 compared with Figure 13 and Figure 14).

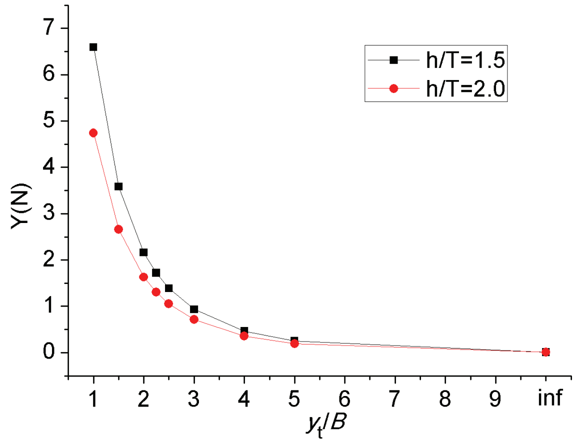

(a) sway force

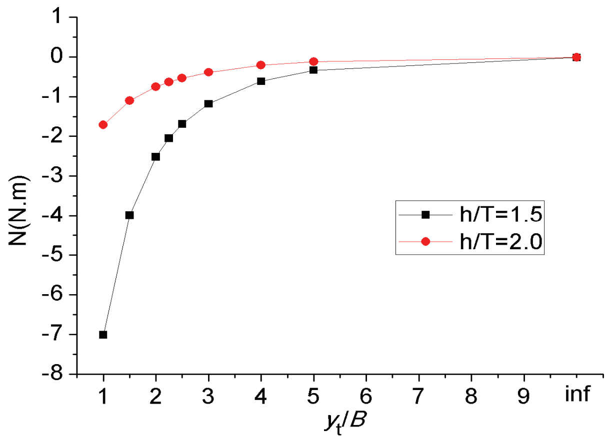

(b) yaw moment

Figure 17 Sway force and yaw moment at different water depths with δ=0°

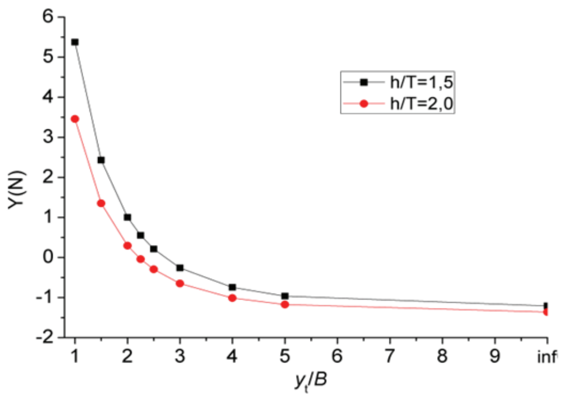

(a) sway force

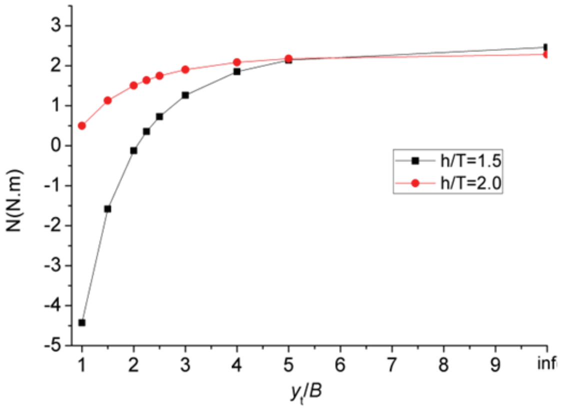

(b) yaw moment

Figure 18 Sway force and yaw moment at different water depths with δ=15°

As shown in Figure 18, when δ=15°, the influence of water depth on sway force and yaw moment is generally similar to that when δ=0°. The yaw moment curves intersect when the distance of ship to bank is relatively large (y_t/B=5~6), which means the bank effect becomes weaker and the rudder effect becomes dominant. This can be explained by flow field as in section 4.2(a), case (2) when the rudder angle is positive.

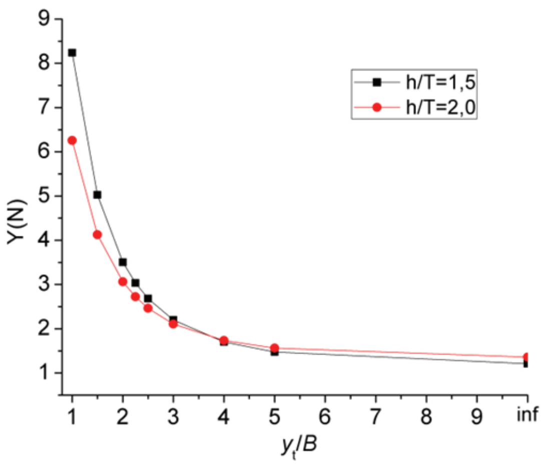

(a) sway force

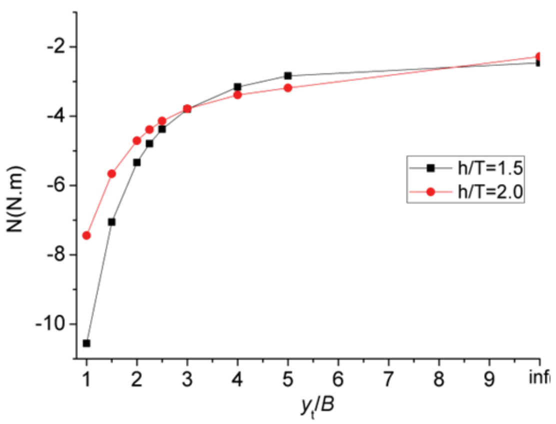

(b) yaw moment

Figure 19 Sway force and yaw moment at different water depths with δ=−15°

As shown in Figure 19, when δ=−15°, the force and moment change more complicated with the decrease of the ship-bank distance: the main change tendency is similar to that when δ=0° or 15°, but both the sway force and yaw moment curves at the two water depths intersect. For the yaw moment curves, the intersection happens more than once. This can also be explained by the flow field in section 4.2(a), case (3) when the rudder angle is negative.

Figure 20 shows the critical state described by curves $Y(y_t,\delta)=0$ and $N(y_t,\delta)=0$ for the two water depths. It can be seen that curves $Y=0$ and $N=0$ for h/T=2.0 move down and to the left compared with those for h/T=1.5, resulting in that the area of Y<0 and N>0 is much larger at h/T=2.0 than that at h/T=1.5, while the area of Y>0 and N<0 is much smaller.

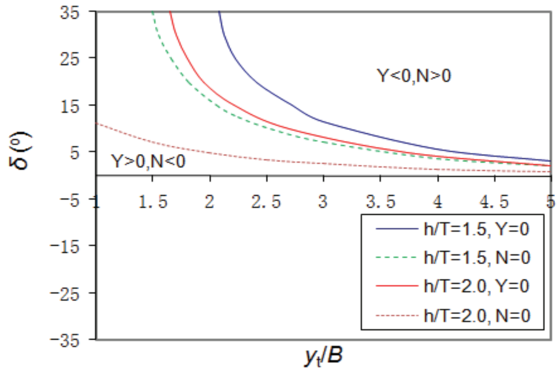

Figure 20 Curves indicating the critical state at different water depths

5. CONCLUSIONS

In this paper, CFD method is applied to numerically simulate the viscous flow around a ship appended with a rudder sailing along a bank in shallow water. Numerical study is carried out for a KCS hull appended with a semi-balanced horn rudder. A series of calculations for the hull-rudder system sailing with different rudder angles at different ship-bank distances are performed. The flow field features and the hydrodynamic force and moment of the hull-rudder system are analysed. From this study the following conclusions can be drawn:

The bank effect for a ship sailing along a bank can be predicted numerically. Since all the shape and size of the channel, the form and location of the ship and rudder can be modified conveniently in the CFD simulation, the analysis on the influences of these factors is facilitated greatly.

The bank effect becomes larger with the decrease of the ship-bank distance. At a certain ship-bank distance, the hydrodynamic force and moment become larger with the increase of rudder angle turning away from the bank. On the other hand, they become smaller or even change to the opposite direction with the increase of rudder angle turning to the bank, which indicates that the rudder effect could counteract the bank effect to some extent.

By comparing the flow field and hydrodynamic forces on the hull-rudder system at different water depths, it can be seen that the bank effect is stronger in shallower water, while the rudder effect is stronger in deep water. The influence of water depth on the overall hydrodynamics of the hull-rudder system can be complex.

The hydrodynamic analysis implemented in this study could provide some guidance for steering a ship traveling ahead along a bank in shallow water to ensure the safe navigation. Future study will focus on the influence of drift angle, ship squat and propeller out-stream.

6. ACKNOWLEDGEMENTS

This work is supported by the National Natural Science Foundation of China (Grant Nos. 51061130548, 51179019).

7. REFERENCES

1. NORRBIN, N. H., Bank Effects on a Ship Moving Through a Short Dredged Channel, *10th Symposium on Naval Hydrodynamics*, *Washington, USA, pp.71-88*, 1974.
2. NORRBIN, N.H., Bank Clearance and Optimal Section Shape for Ship Canals, *Proceedings of 26th PIANC International Navigation Congress*, *Brussels, Belgium, pp.167-178*, 1985.
3. RENILSON, M.R., MUNRO, A., The Effect of Shape and Angle on Bank Interaction, *The Naval Architect*, *pp.E111-E112,* 1989.
4. CH'NG, P.W., DOCTORS, L.J., RENILSON, M.R., A Method of Calculating the Ship-bank Interaction Forces and Moments in Restricted Water, *International Shipbuilding Progress*, *No.421, pp.7-23,* 1993.
5. LI, D. Q., LEER-ANDERSEN, M., OTTOSSON, P., TRÄGÅRDH, P., Experimental Investigation of Bank Effects under Extreme Conditions, *Proceedings of* 8th *International Symposium on Practical Design of Ships and Other Floating Structures, PRADS2001, Shanghai, China, pp.541-546*, 2001.
6. DUFFY, J.T., The Effect of Channel Geometry on Ship Operation in a Port, *Proceedings of* 30th *PIANC-AIPCN Congress, Sydney, Australia*, 2002.
7. VANTORRE, M., DELEFORTRIE, G., ELOOT, K. and LAFORCE, E., Experimental Investigation of Ship-Bank Interaction Forces, *Proceedings of International Conference on Marine Simulation and Ship Maneuverability, MARSIM 2003, Kanazawa, Japan, pp.RC-31-1-RC-31-9*, 2003.
8. LATAIRE, E. and VANTORRE, M., Ship-Bank Interaction Induced by Irregular Bank Geometries, *27th Symposium on Naval Hydrodynamics*, 2008.
9. MIAO, Q.M., XIA, J.Z., CHWANG, A.T. and DUFFY, J., Numerical Study of Bank Effects on a Ship Travelling in a Channel, *Proceedings of* 8th *International Conference on Numerical Ship Hydrodynamics*, 2003.
10. YAO, J.X., ZOU, Z.J., Calculation of Ship Squat in Restricted Waterways by Using a 3-D Panel Method, *9th International Conference on Hydrodynamics*, *ICHD 2010, Shanghai, China,* 2010.
11. LO, D. C., SU, Dong-Taur and CHEN Jan-Ming., Application of Computational Fluid Dynamics Simulations to the Analysis of Bank Effects in Restricted Waters, *Journal of Navigation, 62, pp.477-491,* 2009.
12. WANG, H. M., ZOU, Z. J., XIE, Y. H., KONG, W. L., Numerical Study of Viscous Hydrodynamic Forces on a Ship Navigating near Bank in Shallow Water, *20th International Offshore and Polar Engineering Conference, ISOPE2010, Beijing, China*, 2010.
13. ZOU, L., LARSSON, L., DELEFORTRIE, G. and LATAIRE, E., CFD Prediction and Validation of Ship-bank Interaction in a Canal, *2nd International Conference on Ship Manoeuvring in Shallow and Confined Water: Ship to Ship Interaction, Trondheim, Norway, pp.413-422,* 2011.
14. ELOOT, K., VERWILLIGEN, J., VANTORRE, M., A Methodology for Evaluating the Controllability of a Ship Navigating in a Restricted Channel, *Archives of Civil and Mechanical Engineering, Volume VII, pp.91-104*, 2007.
15. FERZIGER J. H. and PERIC M. Computational Methods for Fluid Dynamics. *New York: Springer-Verlag*, 1996.
16. ANSYS Inc., ANASYS FLUENT Theory Guide 14.0, *ANSYS Inc., November 2011.*
17. ITTC, Recommended Procedures and Guidelines: Practical Guidelines for Ship CFD Applications, *ITTC Procedures No. 7.5-03-02-03, August 2011.*
18. ANSYS Inc., ANASYS FLUENT Users' Guide 14.0, *ANSYS Inc., November 2011.*
19. SIMMAN 2008, *Workshop on Verification and Validation of Ship Maneuvering Simulation Methods, Copenhagen, Denmark, www.simman2008.dk*, 2008.

